EURASIP Journal on Applied Signal Processing 2005:5, 743–756

Generalized Multicarrier CDMA: Unification and Linear Equalization

Georgios B. Giannakis
Department of Electrical and Computer Engineering, University of Minnesota, 200 Union Street SE, Minneapolis, MN 55455, USA
Email: georgios@ece.umn.edu

Paul A. Anghel
Department of Electrical and Computer Engineering, University of Minnesota, 200 Union Street SE, Minneapolis, MN 55455, USA
Email: panghel@ece.umn.edu

Zhengdao Wang
Department of Electrical and Computer Engineering, Iowa State University, 2215 Coover Hall, Ames, IA 50011, USA
Email: zhengdao@iastate.edu

Received 11 August 2003; Revised 21 January 2004

Relying on block-symbol spreading and judicious design of user codes, this paper builds on the generalized multicarrier (GMC) quasisynchronous CDMA system that is capable of multiuser interference (MUI) elimination and intersymbol interference (ISI) suppression with guaranteed symbol recovery, regardless of the wireless frequency-selective channels. GMC-CDMA affords an all-digital unifying framework, which encompasses single-carrier and several multicarrier (MC) CDMA systems. Besides the unifying framework, it is shown that GMC-CDMA offers flexibility both in full load (maximum number of users allowed by the available bandwidth) and in reduced load settings. A novel blind channel estimation algorithm is also derived. Analytical evaluation and simulations illustrate the superior error performance and flexibility of uncoded GMC-CDMA over competing MC-CDMA alternatives especially in the presence of uplink multipath channels.

Keywords and phrases: multicarrier CDMA, multipath fading channels, blind equalization.

1. INTRODUCTION

Mitigation of frequency-selective multipath and elimination of multiuser interference (MUI) have received considerable attention as they constitute the main limiting performance factors in wireless CDMA systems. Orthogonal frequency-division multiple access (OFDMA) [1], the multiuser counterpart of orthogonal frequency-division multiplexing (OFDM) [2], is capable of complete MUI elimination in the downlink provided that a sufficiently long cyclic prefix is used at the transmitter. However, plain OFDMA cannot collect multipath diversity and therefore suffers from frequency-selective fading. Alternatives like OFDMA with frequency hopping and/or channel coding [1, pages 213–228] have been proposed to increase frequency diversity and therefore enhance robustness to multipath, at the price of increased complexity and/or reduced bandwidth efficiency. Multicarrier (MC) CDMA systems have been developed to capitalize on both OFDMA's resilience to MUI and direct-sequence (DS) CDMA's robustness against frequency selectivity to mitigate both MUI and the intersymbol interference (ISI) caused by time-dispersive channels [3, 4, 5, 6, 7, 8, 9]. The spread-spectrum multicarrier multiple-access schemes developed in [6, 10, 11] rely on bandwidth-expanding repetition or convolutional codes for MUI elimination and mitigation of frequency-selective uplink channels. But no existing MC- or DS-CDMA scheme guarantees (blind or not) linear equalizability in the uplink with uncoded transmissions and without imposing constraints on the (possibly unknown) multipath channel nulls.

Recently, the so-called AMOUR system of [12] has introduced generalized multicarrier transceivers for the uplink that eliminate MUI deterministically and guarantee finite impulse response (FIR) channel-irrespective symbol recovery of uncoded transmissions with FIR equalizers. The system of [12] incorporates an algorithm for blind channel estimation and equalization that exploits the redundancy in the precoded transmissions, has low (linear) complexity, and does not trade bandwidth efficiency for lowering the exponential complexity of maximum-likelihood receivers as in [10].

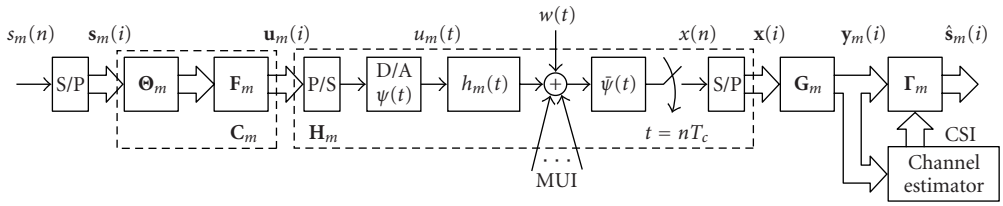

Figure 1: Continuous- and discrete-time equivalent multichannel model.

We deal in this paper with a generalized multicarrier (GMC) CDMA system offering the same features as the system in [12], but with the following additional novelties.

(i) It provides an all-digital unification of various CDMA schemes proposed in the literature, including the conventional (single-carrier) direct-sequence CDMA (DS-CDMA), multicarrier CDMA (MC-CDMA), multicarrier direct-sequence CDMA (MC-DS-CDMA), and multitone CDMA (MT-CDMA). Relying on this unification, GMC-CDMA enables all-digital software radio implementation of different schemes by simply adjusting the spreading-code matrix entries, which in turn facilitates seamless interoperability of different multicarrier wireless service providers.

(ii) It reveals the symbol recovery problem the existing single-carrier and multicarrier CDMA schemes suffer from in the uplink and in some cases also in the downlink. Such problems relate to channel invertibility and lead to considerable loss in error performance. For random (or time-varying) frequency-selective channels, loss of symbol recovery is equivalent to loss of multipath diversity [13].

(iii) It develops a novel blind channel estimation algorithm for a wide class of linearly precoded transmissions that guarantees channel- and constellation-irrespective symbol recovery. While the blind channel estimation algorithm developed in this paper applies to a class that includes Vandermonde, pseudorandom noise, and Walsh-Hadamard precoders as special cases, existing blind algorithms [12, 14] only work for Vandermonde precoders that give rise to Toeplitz channel matrices.

(iv) It introduces frequency reallocation for underloaded GMC-CDMA systems that preserve MUI/ISI-free properties. It also shows how the frequency reallocation preserves the symbol recovery property and it illustrates how the error performance is affected by the reallocation. Current DS-CDMA technology achieves a typical bandwidth efficiency of 25% [15]. Therefore, multiple-access schemes with improved utilization of resources (in our case, the subcarriers) have considerable practical impact. Preserving the MUI/ISI-free properties offers the benefits of blind channel estimation, maximum diversity order in random multipath fading channels [13] and therefore improved error performance.

The paper is organized as follows. The baseband chip-rate sampled model for a GMC-CDMA system is presented in Section 2. In Section 3, it is shown how GMC-CDMA can be reverted to DS-CDMA or existing and novel variants of MC-CDMA systems. Based on this unifying all-digital model, GMC-CDMA's MUI eliminating precoders and decoders for variable load are developed in Section 4. In Section 5, the blind channel estimation algorithm is derived. Section 6 is concerned with bandwidth distribution for reduced-load setups. Simulations are presented in Section 7, and Section 8 is reserved for concluding remarks.

We adopt the following notational conventions. Bold upper (lower) case letters denote matrices (column vectors). An upper case subscript associated with a matrix or vector denotes its dimension. A $J \times J$ identity matrix is denoted by $\mathbf{I}_J$ and the all-zero matrix of size $K \times J$ is denoted as $\mathbf{0}_{K\times J}$. Superscript $\mathcal{H}$ will stand for Hermitian, T for transpose, $*$ for conjugate, $\dagger$ for pseudoinverse. We let $\lceil\cdot\rceil$ denote the integer ceil, $\lfloor\cdot\rfloor$ the integer floor, $\otimes$ the Kronecker product, $\mathcal{R}$ the range, $\mathcal{N}$ the null space, and $\delta(i)$ the Kronecker delta; $\mathrm{E}\{\cdot\}$ stands for the ensemble average operator.

2. SYSTEM MODEL

The baseband discrete-time equivalent transmitter and receiver model for the mth user is depicted in Figure 1, where $m \in [0, M-1]$ and M is the number of *active* users out of a maximum $M_{\max}$ users that can be accommodated by the available bandwidth. The information symbol stream $s_m(n)$ with symbol rate $1/T$ is first serial-to-parallel (S/P) converted to form blocks $\mathbf{s}_m(i)$ of size $K \times 1$ with the kth entry of the mth user's ith block denoted as $s_{m,k}(i) := s_m(k + iK)$, $k \in [0, K-1]$. Each of the $\mathbf{s}_m(i)$ blocks is multiplied by a $J \times K$ ($J > K$) tall matrix $\mathbf{\Theta}_m$, which introduces redundancy and spreads the K symbols in $\mathbf{s}_m(i)$ to yield precoded blocks of size J. Matrix $\mathbf{\Theta}_m$ can be viewed as an "inner code" that will facilitate ISI suppression, while the subsequent redundant precoder described by the tall $P \times J$ ($P > J$) matrix $\mathbf{F}_m$ constitutes an "outer code" that will accomplish MUI elimination. The combined linear block-code $\mathbf{C}_m := \mathbf{F}_m\mathbf{\Theta}_m$ operates over the complex field. Uncoded GMC-CDMA transmissions do not include a channel encoder over the Galois field, but if present, the encoder should precede the $\mathbf{C}_m$ block.

The precoded $P \times 1$ vector of chip samples

$$\mathbf{u}_m(i) := \mathbf{F}_m\mathbf{\Theta}_m\mathbf{s}_m(i) = \mathbf{C}_m\mathbf{s}_m(i) \tag{1}$$

is first parallel-to-serial (P/S) and then digital-to-analog (D/A) converted using a chip waveform $\psi(t)$, to yield the continuous-time signal $u_m(t) = \sum_{n=-\infty}^{+\infty} \sum_{k=0}^{K-1} \sum_{i=-\infty}^{+\infty} s_{m,k}(i) c_{m,k}(n - iP)\psi(t - nT_c)$, where $c_{m,k}(p)$ is the $(p+1, k+1)$th entry of the $P \times K$ matrix $\mathbf{C}_m$. Next, $u_m(t)$ is transmitted through the frequency-selective channel $h_m(t)$. Although we focus on the uplink, the downlink is subsumed by our model (it corresponds to having $h_m(t) = h(t)$ for all m). The resulting aggregate signal $x(t)$ from all active users is filtered by a square-root Nyquist receive filter $\bar{\psi}(t)$, and then sampled at the chip rate $1/T_c$. Next, the sampled signal $x(n)$ is serial-to-parallel converted and processed by the all-digital chip-sampled multichannel receiver $\mathbf{G}_m$.

We denote by $h_m(n)$, $n \in [0, L]$, the taps of the mth user's discrete chip-rate sampled FIR channel that we assume to have known maximum order L for all m. We consider a *quasisynchronous* model which allows for *bounded* (and preferably small) relative delays among users and we incorporate the maximum relative delay among users in the maximum channel order L. Specifically, with maximum relative delay $\tau_{\max,d}$ among the users and maximum delay spread $\tau_{\max,s}$, the chip-sampled discrete-time equivalent channel order is $L = \lceil (\tau_{\max,d} + \tau_{\max,s})/T_c \rceil$. Because mobile users attempt to synchronize with the base station's pilot waveform, the asynchronism between users is bounded and can be assumed to span only a few chips. Since deterministic MUI elimination is facilitated by assuming quasisynchronous transmissions, in principle, quasisynchronism replaces power control by delay control.

Selecting the transmitted block length $P > L$, $\mathbf{u}_m(i)$ propagates through an equivalent channel described by $\mathbf{H}_m \delta(i) + \mathbf{H}_m^{(1)} \delta(i-1)$, where $\mathbf{H}_m$ is a $P \times P$ lower triangular Toeplitz matrix with (n, p)th entry $h_m(n - p)$ and $\mathbf{H}_m^{(1)}$ is a $P \times P$ upper triangular Toeplitz matrix with (n, p)th entry $h_m(n - p + P)$.

To avoid channel-induced interblock interference (IBI) introduced by $\mathbf{H}_m^{(1)}$, we design our transmitted blocks $\mathbf{u}_m(i)$ for all i to have L zeros (guard chips) so that $\mathbf{H}_m^{(1)} \mathbf{u}_m(i) = \mathbf{0}_{P \times 1}$. Specifically, we construct our $P \times J$ precoders $\mathbf{F}_m$ with trailing zeros.

Trailing zeros (TZ)

The $L \times J$ lower submatrix of $\mathbf{F}_m$ is set to zero.

The trailing zeros at the transmitter can be replaced by the so-called cyclic prefix.

Cyclic prefix (CP)

Our block precoders $\mathbf{F}_m$ are designed such that their $L \times J$ top and bottom submatrices are identical. Similar to OFDM, the CP must be discarded at the receiver by setting the first L columns of $\mathbf{G}_m$ to zero in order to eliminate IBI (see also [12, 16, 17]).

With TZ transmissions, the received $P \times 1$ IBI-free vector $\mathbf{x}(i)$ in additive Gaussian noise (AGN) $\mathbf{w}(i)$ is expressed as

$$\mathbf{x}(i) = \sum_{m=0}^{M-1} \mathbf{H}_m \mathbf{C}_m \mathbf{s}_m(i) + \mathbf{w}(i). \tag{2}$$

Processing $\mathbf{x}(i)$ by the mth user's multichannel receiver amounts to multiplying it with the $J \times P$ matrix $\mathbf{G}_m$ that eliminates MUI to yield $\mathbf{y}_m(i) = \mathbf{G}_m \mathbf{x}(i)$. Similar to [12], the precoder/decoder matrices $\{\mathbf{F}_m, \mathbf{G}_m\}$ will be designed such that MUI is eliminated from $\mathbf{x}(i)$ regardless of the channels $\mathbf{H}_m$. Channel state information (CSI) acquired from the channel estimator (see Figure 1) will be used to specify the linear equalizer $\mathbf{\Gamma}_m$ which removes ISI from the MUI-free signals $\mathbf{y}_m(i)$ to obtain the estimated symbols $\hat{\mathbf{s}}_m(i) = \mathbf{\Gamma}_m \mathbf{G}_m \mathbf{x}(i)$ that are passed on to the decision device.

Before we design such precoders/decoders for a variable-load system, we first establish the unifying character of our digital block-spreading system.

3. ALL-DIGITAL UNIFICATION OF MULTICARRIER CDMA

A number of multiple-access schemes fall under the model of Figure 1. A *single-carrier* DS-CDMA system with processing gain $P - L$ and TZ transmissions can be implemented with our model by setting $K = 1$, in which case no symbol blocking occurs at the transmitter. The block-spreading code $\mathbf{C}_m$ in (1) is then replaced by the $P \times 1$ symbol-periodic spreading vector $\mathbf{c}_m := [c_m(0) \ \cdots \ c_m(P-L-1) \ 0 \ \cdots \ 0]^T$ with its first $P - L$ entries taken from Gold, Walsh-Hadamard (WH), or ± 1 pseudonoise (PN) sequences. If the DS-CDMA spreading code does not have a TZ structure, there will be IBI (and thus ISI) in the received signal which is given by $\mathbf{x}(i) = \sum_{m=0}^{M-1} [\mathbf{H}_m \mathbf{c}_m s_m(i) + \mathbf{H}_m^{(1)} \mathbf{c}_m s_m(i-1)] + \mathbf{w}(i)$.

DS-CDMA cannot guarantee channel-irrespective symbol recovery in the uplink [16]. For instance, there may exist channels for which signals received from two different users cancel each other. Specifically, consider a user m with code $\mathbf{c}_m = [1, 1, 0]^T$ ($P = 3$), and channel $h_m(n) = \delta(n) - \delta(n-1)$ superimposed on a user $\mu \neq m$ with code $\mathbf{c}_\mu = [1, -1, 0]^T$, and channel $h_\mu(n) = \delta(n) + \delta(n-1)$. Let these two users transmit the symbols $s_m(n) = 1$ and $s_\mu(n) = -1$ for some n. Then, the mth user's received signal $x_m(n)$ cancels the μth user's received signal $x_\mu(n)$, as $x_m(n) = \delta(n) - \delta(n-2) = -x_\mu(n)$. This renders recovery of $s_m(n)$ and $s_\mu(n)$ from $x_m(n) + x_\mu(n)$ impossible even with maximum-likelihood multiuser detection.

In the sequel, we will also show how three popular multicarrier transmissions can be implemented digitally as special cases of GMC-CDMA. With their discrete-time equivalent models, it will become clear that none of them guarantees symbol recovery in the uplink, although recovery is possible in the downlink after appropriate modifications.

3.1. Multicarrier CDMA

MC-CDMA (a.k.a. CDMA-OFDM [4, 18]) combines DS-CDMA with OFDM modulation. Every MC-CDMA user spreads each symbol with a symbol-periodic DS sequence which is subsequently modulated by OFDM using the inverse fast fourier transform (IFFT) as in [2]. No symbol blocking occurs at the transmitter (i.e., $K = 1$) and $\mathbf{\Theta}_m$ is a $J \times 1$ vector $\boldsymbol{\theta}_m$ (the spreading sequence). Unlike (1), the $\mathbf{F}_m$ matrix is no longer user-specific. With $P = J + L$,

the outer code $\mathbf{F}_m$ (here denoted as $\mathbf{F}_{\text{cp}}$) is selected to be a $P \times J$ matrix consisting of a $J \times J$ IFFT matrix $\mathbf{F}_J$ with $(i+1,k+1)$th entry $(1/\sqrt{J})\exp(j2\pi ik/J)$, augmented on the top by an $L \times J$ matrix that replicates the last L rows of $\mathbf{F}_J$ and inserts the CP. At the receiver, the CP is discarded by choosing $\mathbf{G}_m = \mathbf{G}_{\text{cp}} := [\mathbf{0}_{J\times L}, \mathbf{F}_J^{\mathcal{H}}]$ for all m, where $\mathbf{0}_{J\times L}$ eliminates the CP (and thus IBI) while $\mathbf{F}_J^{\mathcal{H}}$ performs fast Fourier transform (FFT) processing of the received blocks. This selection of outer-precoder-decoder matrices $\{\mathbf{F}_m, \mathbf{G}_m\} = \{\mathbf{F}_{\text{cp}}, \mathbf{G}_{\text{cp}}\}$ does not cancel MUI. However, IFFT at the transmitter and FFT of the IBI-free blocks at the receiver convert the frequency-selective channel (described by the $P \times P$ Toeplitz matrix $\mathbf{H}_m$ in (2)) to flat fading subchannels represented by the $J \times J$ diagonal matrix $\mathbf{D}_m(H) := \mathbf{G}_{\text{cp}}\mathbf{H}_m\mathbf{F}_{\text{cp}} = \text{diag}[H_m(e^{j0}) \cdots H_m(e^{j2\pi(J-1)/J})]$ with the amplitude of the $(i+1,i+1)$th entry $H_m(e^{j2\pi i/J}) := \sum_{l=0}^{L} h_m(l)\exp(-j2\pi il/J)$ representing the scalar attenuation of the ith suntanned. The nth IBI-free FFT processed block at the receiver can then be written as

$$\mathbf{y}(i) := \mathbf{G}_{\text{cp}}\mathbf{x}(i) = \sum_{m=0}^{M-1} \mathbf{D}_m(H)\boldsymbol{\theta}_m s_m(i) + \mathbf{G}_{\text{cp}}\mathbf{w}(i). \quad (3)$$

It follows from (3) that recovery of $s_m(i)$ for uplink or downlink transmissions is not always possible. As a counterexample for the downlink, we take a user m with WH code $\boldsymbol{\theta}_m = [1,1,1,1]^T$ ($J = 4$) and a user μ with WH code $\boldsymbol{\theta}_\mu = [1,-1,1,-1]^T$. Suppose that both users experience the same downlink channel $h(n) = \delta(n)+\delta(n-2)$. It can be verified by direct substitution that $\mathbf{D}_m(H)\boldsymbol{\theta}_m = \mathbf{D}_\mu(H)\boldsymbol{\theta}_\mu = [2,0,2,0]^T$, which implies that it is impossible to decide what each of the two users transmits.

Instead of the CP, we can also extend $\mathbf{F}_J$ with an $L \times J$ all-zero matrix at the bottom, which amounts to padding the transmission with TZ. In this case, $\mathbf{F}_m = \mathbf{F}_{\text{tz}} := [\mathbf{F}_J, \mathbf{0}_{J\times L}]^T$ for all m, and we can write $\mathbf{H}_m\mathbf{F}_{\text{tz}} = \tilde{\mathbf{H}}_m\mathbf{F}_J$, where $\tilde{\mathbf{H}}_m$ is formed by the first J columns of $\mathbf{H}_m$ and is always full rank thanks to its Toeplitz structure as long as $h_m(n) \neq 0$ for at least one $n \in [0,L]$. Interestingly, for this MC-CDMA with zero-padded transmissions, the received block in (2) without FFT processing at the receiver can be written as

$$\mathbf{x}(i) = \sum_{m=0}^{M-1} \mathbf{H}_m\mathbf{F}_{\text{tz}}\boldsymbol{\theta}_m s_m(i) + \mathbf{w}(i) = \sum_{m=0}^{M-1} \tilde{\mathbf{H}}_m\mathbf{F}_J\boldsymbol{\theta}_m s_m(i) + \mathbf{w}(i). \quad (4)$$

We show in Appendix A that if the despreading matrix $\mathbf{G}_m = \mathbf{G}_{\text{tz}}^{(1)}$ for all m is selected to be a fat $J \times P$ FFT matrix with $(k+1,p+1)$th entry $(1/\sqrt{J})\exp(-j2\pi kp/J)$, then $\mathbf{y}(i) := \mathbf{G}_{\text{tz}}^{(1)}\mathbf{x}(i)$ coincides with (3) if we consider a noiseless setup, that is, $\mathbf{w}(i) = \mathbf{0}_{P\times 1}$. Similar to (3), symbol recovery is not assured either.

However, going back to (4), we observe that for TZ-MC-CDMA constellation-irrespective recovery (in a noiseless scenario) of $\{s_m(i)\}_{m=0}^{M-1}$ is accomplished if the $P \times M$ matrix $\boldsymbol{\Omega} := [\tilde{\mathbf{H}}_0\mathbf{F}_J\boldsymbol{\theta}_0, \ldots, \tilde{\mathbf{H}}_{M-1}\mathbf{F}_J\boldsymbol{\theta}_{M-1}]$ is guaranteed to be invertible from the left.

In the *downlink*, $\tilde{\mathbf{H}}_m$ is common to all the users (i.e., $\tilde{\mathbf{H}}_m = \tilde{\mathbf{H}}$ for all m), which implies $\boldsymbol{\Omega} = \tilde{\mathbf{H}}\mathbf{F}_J[\boldsymbol{\theta}_0, \ldots, \boldsymbol{\theta}_{M-1}]$. Since both $\tilde{\mathbf{H}}$ and $\mathbf{F}_J$ have full column rank, we conclude that $\tilde{\mathbf{H}}\mathbf{F}_J$ is left invertible. If the vectors $\{\boldsymbol{\theta}_m\}_{m=0}^{M-1}$ are designed to be linearly independent, the symbols $\{s_m(i)\}_{m=0}^{M-1}$ can be recovered at the receiver by premultiplying $\mathbf{x}(i)$ in (4) with $\mathbf{G}_{\text{tz}}^{(2)} := \boldsymbol{\Omega}^\dagger$. To obtain estimates for the mth user's symbols $s_m(i)$, only, we select $\boldsymbol{\Gamma}_m$ to be a $1 \times M$ vector $\boldsymbol{\gamma}_m^T$ equal to the mth row of the identity matrix $\mathbf{I}_M$. Hence, unlike MC-CDMA with CP, MC-CDMA with TZ guarantees symbol recovery in the downlink.

For the *uplink* however, symbol recovery is not guaranteed even with TZ-MC-CDMA. As a counterexample, consider user m with a WH code $\boldsymbol{\theta}_m = [1,1,1,1]^T$, channel $h_m(n) = \delta(n-2)$ superimposed on a user μ with WH code $\boldsymbol{\theta}_\mu = [1,-1,1,-1]^T$, and channel $h_\mu(n) = \delta(n)$. Because $\tilde{\mathbf{H}}_m\mathbf{F}_J\boldsymbol{\theta}_m = \tilde{\mathbf{H}}_\mu\mathbf{F}_J\boldsymbol{\theta}_\mu = [0,0,4,0,0,0]^T$, matrix $\boldsymbol{\Omega}$ has two identical columns; hence, it is not full column rank which verifies that even with TZ, symbol recovery is not always assured in uplink MC-CDMA.

If the guarantees on symbol recovery in the downlink can be traded for lowering the receiver's complexity, then instead of processing $\mathbf{x}(i)$ in (4) with $\mathbf{G}_{\text{tz}}^{(2)}$, one can use orthogonal codes $\{\boldsymbol{\theta}_m\}_{m=0}^{M}$ for either CP or TZ transmissions. Demodulation of $\mathbf{y}(i)$ in (3) can then be accomplished using the zero-forcing (ZF) detector of [4] which amounts to choosing $\boldsymbol{\gamma}_m^T = \boldsymbol{\theta}_m^T\mathbf{D}_m^\dagger(H)$, provided that the multiuser channel is available at the receiver. MC-CDMA requires a more complex channel estimation algorithm especially in the uplink (see [10] and references therein) relative to systems that can guarantee MUI-free reception regardless of multipath [10, 12].

3.2. Multicarrier DS-CDMA

In MC-DS-CDMA, the mth user's information symbol stream $s_m(n)$ with rate $1/T$ is S/P converted to K substreams $\{s_{m,k}(i)\}_{k=0}^{K-1}$ each with rate $1/(KT)$. Each substream is D/A converted and then spread by a Q-long user-specific symbol-periodic code $\theta_m(t)$ (common to all substreams) with chip rate $1/T_{\text{ds}}$ and spectral support B_{ds}. Each of the spread substreams $\{\sum_{i=-\infty}^{+\infty} s_{m,k}(i)\theta_m(t-iKT)\}_{k=0}^{K-1}$, with $KT = QT_{\text{ds}}$, modulates a subcarrier with frequency f_k. After modulation, all signals on the K parallel branches are added to yield the continuous-time transmitted signal

$$u_m(t) = \sum_{k=0}^{K-1}\sum_{i=-\infty}^{+\infty} s_{m,k}(i)\theta_m(t-iKT)e^{j2\pi f_k t} \quad (5)$$

with spectral support $B = B_{\text{ds}} + \sum_{k=1}^{K-1}\Delta f_k$, where Δf_k is the frequency separation between subcarriers f_{k-1} and f_k (see also [3, 5]).

To implement MC-DS-CDMA digitally, we note that the bandlimited $u_m(t)$ can be reconstructed from its samples $u_m(n) := u_m(t)|_{t=n/B}$ using sinc pulses according to the sampling theorem. If the sampling rate ($1/T_c$ in our model) is higher than B, say $f_s := 1/T_c = (1+\beta)B$, $0 < \beta < 1$, then more realistic pulse shapers (e.g., raised cosine) can be

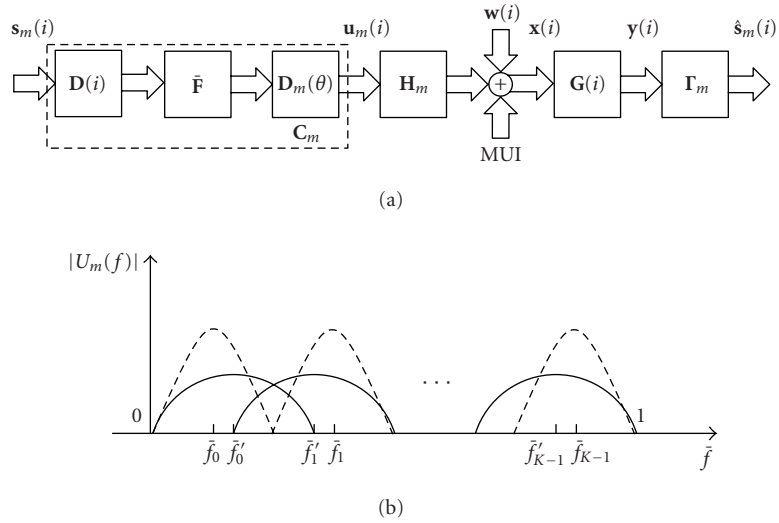

FIGURE 2: MC-DS-CDMA system: (a) digital baseband transceiver model; (b) spectrum of the transmitted signal $\mathbf{u}_m(i)$ for 2 sets of $\{\bar{f}_k\}_{k=0}^{K-1}$.

used to generate $u_m(t)$ from $u_m(n)$. To be specific, we define $\theta_m(n) := \theta_m(t)|_{t=nT_c}$ and $\bar{f}_k = f_k/f_s$. By properly selecting β so that $KTf_s = KT/T_c := P$ is an integer, the sampled spreading code $\theta_m(n)$ will have period P. In this case, with $\psi(t)$ denoting the raised cosine pulse with roll-off factor $\alpha = \beta/(1+\beta)$ and spectral support $(1+\alpha)/T_c$, we can write $u_m(t) = \sum_{n=-\infty}^{+\infty} u_m(n)\psi(t-nT_c)$, where

$$u_m(n) = \sum_{k=0}^{K-1} \sum_{i=-\infty}^{+\infty} s_{m,k}(i)\theta_m(n-iP)e^{j2\pi\bar{f}_k n}. \tag{6}$$

Sampling $u_m(t)$ in (5) every $t = nT_c$ seconds, we find $u_m(n)$ in (6) which proves that one can perform the MC-DS-CDMA modulation by first generating the discrete-time chip-rate sequence $u_m(n)$ and then passing it through the raised cosine filter $\psi(t)$.

To cast (6) in our block-spreading model (1), we define the $K\times K$ diagonal matrix $\mathbf{D}(i) := \text{diag}[e^{j2\pi\bar{f}_0 iP}, \ldots, e^{j2\pi\bar{f}_{K-1}iP}]$ which accounts for the subcarrier phase shifts between two consecutive $\mathbf{u}_m(i)$ blocks of length P. By taking $n = iP + p$, $p \in [0, P-1]$ in (6), we can write the ith transmitted block as

$$\mathbf{u}_m(i) = \mathbf{D}_m(\theta)\bar{\mathbf{F}}\mathbf{D}(i)\mathbf{s}_m(i), \tag{7}$$

where the $P \times P$ outer-spreading code matrix $\mathbf{D}_m(\theta) := \text{diag}[\theta_{m,0}, \ldots, \theta_{m,P-1}]$ is user specific, while the $P \times K$ inner-spreading code matrix $\bar{\mathbf{F}} := [\mathbf{f}_P^*(e^{j2\pi\bar{f}_0}), \ldots, \mathbf{f}_P^*(e^{j2\pi\bar{f}_{K-1}})]$ with $\mathbf{f}_P(z) := [1 \;\; z^{-1} \;\; \cdots \;\; z^{-P+1}]^T$ is common to all users.

Selecting the spreading codes $\boldsymbol{\theta}_m := [\theta_{m,0} \;\; \cdots \;\; \theta_{m,P-1}]$ to have enough ($\geq L$) trailing zeros for IBI suppression, we can obtain the received block $\mathbf{x}(i)$ as in (2) by replacing $\mathbf{C}_m$ with $\mathbf{D}_m(\theta)\bar{\mathbf{F}}\mathbf{D}(i)$ (see also Figure 2):

$$\mathbf{x}(i) = \sum_{m=0}^{M-1} \mathbf{H}_m\mathbf{D}_m(\theta)\bar{\mathbf{F}}\mathbf{D}(i)\mathbf{s}_m(i) + \mathbf{w}(i). \tag{8}$$

At the receiver end, one can process $\mathbf{x}(i)$ using a decorrelating detector $\mathbf{G}(i) = \mathbf{\Omega}^{\dagger}(i)$, where $\mathbf{\Omega}(i) := [\mathbf{H}_0\mathbf{D}_0(\theta)\bar{\mathbf{F}}\mathbf{D}(i), \ldots, \mathbf{H}_{M-1}\mathbf{D}_{M-1}(\theta)\bar{\mathbf{F}}\mathbf{D}(i)]$ in order to obtain estimates of the information symbols $\mathbf{s}_m(i)$ for all active users. Since matrix $\mathbf{\Omega}(i)$ is not always left invertible, we maintain that in MC-DS-CDMA with TZ transmissions symbol recovery is not assured in the uplink. A counterexample can be constructed for $K = 2$ if we let user m have $\mathbf{D}_m(\theta) = \text{diag}[1,1,1,1,0,0]$, channel $h_m(n) = \delta(n) - \exp(j2\pi 2\bar{f}_0)\delta(n-2)$, and user μ have $\mathbf{D}_\mu(\theta) = \text{diag}[1,1,-1,-1,0,0]$ with corresponding channel $h_\mu(n) = \delta(n) + \exp(j2\pi 2\bar{f}_0)\delta(n-2)$. It turns out that for any choice of the carrier frequencies $\{f_k\}_{k=1}^{K-1}$, the matrix $[\mathbf{H}_m\mathbf{D}_m(\theta)\bar{\mathbf{F}}, \mathbf{H}_\mu\mathbf{D}_\mu(\theta)\bar{\mathbf{F}}]$ is not a full column rank and neither is $\mathbf{\Omega}(i)$ for all i. For independent symbols $s_m(n)$, MC-DS-CDMA can be viewed as K parallel DS-CDMA signals, which intuitively explains why, similar to DS-CDMA, symbol recovery can be problematic with uplink channels.

The spectrum of the digital MC-DS-CDMA's transmitted signal $\mathbf{u}_m(i)$ is depicted in Figure 2. We remark that we can increase the overlapping ratio between the spectra of different subcarriers by appropriately choosing $\{\bar{f}_k\}_{k=0}^{K-1}$ to trade off intersubcarrier interference with increased spectral support for the mth user's discrete-time spreading code $\boldsymbol{\theta}_m$.

A special case of MC-DS-CDMA, well known to the literature (see, e.g., [5]), is obtained when $\{f_k = k/T_{\text{ds}}\}_{k=0}^{K-1}$ in which case $\mathbf{D}(i) = \mathbf{I}_K$ for all i. With these subcarrier frequencies, we find $B = B_{\text{ds}} + (K-1)/T_{\text{ds}}$. Using the latter, the block-spreading factor for our discrete-time equivalent model is $P = (1+\beta)KT(B_{\text{ds}} + (K-1)/T_{\text{ds}}) = (1+\beta)(KTB_{\text{ds}} + (K-1)Q)$. Further simplification of the MC-DS-CDMA formulation is possible in this case, if for $t \in [0, QT_{\text{ds}}]$ and $m \in [0, M-1]$, we select the spreading code waveform $\theta_m(t) = \sum_{n=0}^{Q-1} \tilde{\theta}_m(n)\tilde{\psi}(t-nT_{\text{ds}})$, where $\tilde{\boldsymbol{\theta}}_m := [\tilde{\theta}_m(0), \ldots, \tilde{\theta}_m(Q-1)]^T$ is a user dependent Q-long code, and $\tilde{\psi}(t)$ is a rectangular pulse of duration T_{ds}.

Consequently, $B_{\rm ds} = 1/T_{\rm ds}$, and the spectral support of the transmitted MC-DS-CDMA signal in (5) is now $B = K/T_{\rm ds}$ or, after substituting $T_{\rm ds} = KT/Q$, is $B = Q/T$. By sampling at the Nyquist rate, that is, $f_s = B = Q/T$, we obtain a sampled spreading code $\theta_m(n)$ with integer period $P = KTB = KQ$. Since $\theta_m(t)$ is sampled every $T_{\rm ds}/K$, and $\bar{f}_k = k/K$, it turns out in (7) that $\mathbf{D}_m(\theta) = \text{diag}[\bar{\boldsymbol{\theta}}_m \otimes \mathbf{1}_K]$, and $\bar{\mathbf{F}} = \mathbf{1}_Q \otimes \mathbf{F}_K$, where $\mathbf{1}_K$ is an all-one $K \times 1$ vector and $\mathbf{F}_K$ is the $K \times K$ IFFT matrix. We should now use a sinc pulse shaper $\psi(t)$ with spectral support $1/T_c$ to reconstruct the transmitted MC-DS-CDMA signal $u_m(t)$ from $\mathbf{u}_m(i)$. Because $\bar{\mathbf{F}}$ is a rowwise repetition of $K \times K$ IFFT matrices, we remark that if instead of allowing trailing zeros only at the end of $\mathbf{u}_m(i)$ we insert L trailing zeros or a cyclic prefix after each K-symbol block of $\mathbf{u}_m(i)$, we can reduce the complexity of equalization in downlink MC-DS-CDMA with the obvious drawback of reducing spectral efficiency.

3.3. Multitone CDMA

Another special case of MC-DS-CDMA known as MT-CDMA [7] is obtained if the subcarrier frequencies are chosen as $f_k = k/KT$, in which case again $\mathbf{D}(i) = \mathbf{I}_K$ for all i. The continuous-time MT-CDMA's spectral support turns out to be $B = B_{\rm ds} + (K-1)/(KT)$ and therefore $P = (1+\beta)(KTB_{\rm ds} + K - 1)$.

MT-CDMA can offer codes $\boldsymbol{\theta}_m$ with a larger bandwidth than the MC-DS-CDMA of [5] due to a closer subcarrier spacing. But now a smaller frequency shift of the transmitted signal causes spectral leakage between adjacent subcarriers at the receiver, which makes MT-CDMA more susceptible to frequency offsets or Doppler effects encountered with time-varying channels. To better mitigate these effects, one should increase the interspacing between subcarrier frequencies $\bar{f}_k$ and decrease the spreading for each subcarrier. But unlike MC-CDMA, in MC-DS-CDMA, different data symbols ride on different subcarriers. By decreasing subcarrier spreading, recovery of the symbol-modulated subcarriers is more severely affected by channel nulls. Depending on the encountered multipath, one can balance between the amount of spreading allowed per subcarrier and the interspacing of frequencies $\bar{f}_k$ in order to optimize error probability performance.

We have seen in this section that *DS-CDMA, MC-CDMA, MC-DS-CDMA, and MT-CDMA systems can be implemented using our digital GMC-CDMA model.* Although known for OFDMA and MC-CDMA, the novel discrete-time equivalent modeling enables their all-digital implementation within the GMC-CDMA framework. Built on the unification results introduced by [16, 19], our all-digital unification of multicarrier CDMA schemes here clearly demonstrate that in many cases, conventional multicarrier CDMA schemes do not guarantee symbol recovery through frequency-selective multipath uplink channels with linear equalizers even in the absence of noise, which will motivate our GMC designs in the next section. We will prove later in this paper that our GMC designs also guarantee blind identifiability of multiple multipath channels for certain classes of spreading codes.

4. MUI/ISI ELIMINATING GMC CODES

Using the model developed in Section 2, we pursue MUI elimination from $\mathbf{x}(i)$. Relative to [12], we design here block-spreading codes under *variable-load settings* and focus on the role and choice of the inner and outer spreading matrices $\boldsymbol{\Theta}_m$ and $\mathbf{F}_m$. A pertinent choice for $\mathbf{F}_m$ that will facilitate the well sought-after MUI-free reception is

$$\mathbf{F}_m = \mathbf{J}_2\mathbf{F}_{MJ}\mathbf{S}_m := \mathbf{J}_2\mathbf{F}_{MJ}(\mathbf{I}_J \otimes \mathbf{e}_m), \tag{9}$$

where $\mathbf{e}_m$ is the $M \times 1$ standard basis vector with the mth entry equal to 1, while matrix $\mathbf{S}_m := \mathbf{I}_J \otimes \mathbf{e}_m$ selects the mth, $(m+M)$th, $\ldots$, $(m+(J-1)M)$th columns of the $MJ \times MJ$ IFFT matrix $\mathbf{F}_{MJ}$, which is defined such that the $(i+1, k+1)$th entry is $(1/\sqrt{MJ})\exp(j2\pi ik/(MJ))$. The matrix $\mathbf{J}_2 := [\mathbf{I}_{MJ}, \mathbf{0}_{L\times MJ}]^T$ adds L guard chips to $\mathbf{F}_{MJ}\mathbf{S}_m$ and consequently sets the number of rows for precoder $\mathbf{F}_m$ to $P = MJ + L$. Note that even though MJ digital carriers (i.e., columns of $\mathbf{F}_{MJ}$) are available to each user, the selector matrix $\mathbf{S}_m$ allocates J nonoverlapping carriers per user. With this carrier allocation strategy, MUI elimination is achieved by selecting at the receiver

$$\mathbf{G}_m = \left(\mathbf{F}_{MJ}\mathbf{S}_m\right)^{\mathcal{H}}\mathbf{J}_1, \tag{10}$$

where

$$\mathbf{J}_1 := \begin{bmatrix} & \vdots & \\ \mathbf{I}_{MJ} & & \mathbf{I}_L \\ & \vdots & \mathbf{0}_{(MJ-L)\times L} \end{bmatrix}. \tag{11}$$

In order to see why the previous statement is true, we need to observe, after following the proof in Appendix A, that $\mathbf{F}_{MJ}^{\mathcal{H}}\mathbf{J}_1\mathbf{H}_m\mathbf{J}_2\mathbf{F}_{MJ} := \tilde{\mathbf{D}}_m(H_m)$ is an $MJ \times MJ$ diagonal matrix with the nth entry on the diagonal equal to $H_m(\rho^n) := \sum_{l=0}^{L} h_m(l)\rho^{-nl}$, where $\rho := \exp(j2\pi/MJ)$. This allows us to write

$$\mathbf{y}_\mu(i) = \mathbf{G}_\mu\mathbf{x}(i) = \mathbf{S}_\mu^T \sum_{m=0}^{M-1} \tilde{\mathbf{D}}_m(H_m)\mathbf{S}_m\boldsymbol{\Theta}_m\mathbf{s}_m(i) + \boldsymbol{\eta}_\mu(i), \tag{12}$$

where $\boldsymbol{\eta}_\mu(i) := \mathbf{G}_\mu\mathbf{w}(i)$. Because $\mathbf{S}_\mu^T\tilde{\mathbf{D}}_m(H_m)\mathbf{S}_m = \mathbf{0}_J$ for all $m \neq \mu$, $\mathbf{y}_\mu(i)$ is MUI-free. Furthermore,

$$\mathbf{y}_\mu(i) = \mathbf{D}_\mu(H_\mu)\boldsymbol{\Theta}_\mu\mathbf{s}_\mu(i) + \boldsymbol{\eta}_\mu(i), \tag{13}$$

where $\mathbf{D}_\mu(H_\mu) := \mathbf{S}_\mu^T\tilde{\mathbf{D}}_\mu(H_\mu)\mathbf{S}_\mu = \text{diag}[H_\mu(\rho^\mu), H_\mu(\rho^{\mu+M}), \ldots, H_\mu(\rho^{\mu+(J-1)M})]$ is a $J \times J$ diagonal matrix. We want to point out that any set of selector matrices $\{\mathbf{S}_m\}_{m=0}^{M-1}$ that satisfies $\mathbf{S}_\mu^T\tilde{\mathbf{D}}_m(H_m)\mathbf{S}_m = \mathbf{0}_J$ for all $m \neq \mu$ allows for MUI elimination. For example, instead of $\mathbf{S}_m = \mathbf{I}_J \otimes \mathbf{e}_m$, one could select $\mathbf{S}_m = \mathbf{e}_m \otimes \mathbf{I}_J$ and consequently the mth group of J adjacent carriers would be allocated to user m. This works to our advantage since $\{\mathbf{S}_m\}_{m=0}^{M-1}$ and $\{\boldsymbol{\Theta}_m\}_{m=0}^{M-1}$ could be jointly optimized to improve the bit error rate performance or the capacity of the system. However, designing optimal carrier allocation strategies goes beyond the scope of this paper and the reader is referred to [20, 21] for insights on how to select and load different carriers.

With outer-spreading and despreading matrices $\mathbf{F}_\mu$ and $\mathbf{G}_\mu$ as in (9) and (10), we have eliminated MUI and reduced the multiuser detection problem to M single-user symbol recovery problems as in (13). Clearly, not every inner-spreading matrix is qualified for recovering $\mathbf{s}_\mu(i)$ from $\mathbf{y}_\mu(i)$; for example, selecting $\mathbf{\Theta}_\mu = \mathbf{0}_{J\times K}$ would disable recovery. With $\mathbb{C}^K$ denoting the vector space of complex K-tuples, we design $\mathbf{\Theta}_\mu$ in (13) to satisfy the following.

(d1) *$J \geq K + L$ and any $J - L$ rows of $\mathbf{\Theta}_\mu$ span the $\mathbb{C}^K$ row vector space.*

Notice that (d1) can always be checked and enforced at the transmitter. Under (d1), $\mathbf{D}_\mu(H_\mu)\mathbf{\Theta}_\mu$ in (13) will always be full rank, because the added redundancy ($\geq L$) can afford even L diagonal entries of $\mathbf{D}_\mu(H_\mu)$ to be zero (recall that $H_\mu(z)$ has maximum order L and thus at most L nulls). Therefore, identifiability of $\mathbf{s}_\mu(i)$ with linear equalizers can be guaranteed regardless of the multipath channel $\{h_\mu(l)\}_{l=0}^L$ and the adopted signal constellation. Although decision-directed alternatives are possible at high signal-to-noise ratio (SNR), constellation-irrespective linear equalizers are computationally attractive, they avoid catastrophic error propagation at low SNR and allow for variable bit-loading transmissions. Furthermore, minimum redundancy transmissions with guaranteed symbol recovery are assured if we choose $J = J_{\min} := K + L$, which leads to a transmitted block of size $P = M(K + L) + L$. Possible choices for $\mathbf{\Theta}_\mu$ that are flexible enough for our design include

(i) Vandermonde spreading (Va-S): the $J \times K$ Vandermonde matrix $\mathbf{\Theta}_\mu := [\mathbf{f}_K(\rho^\mu), \mathbf{f}_K(\rho^{\mu+M}), \ldots, \mathbf{f}_K(\rho^{\mu+(J-1)M})]^T$, used in the AMOUR system [12];

(ii) Walsh-Hadamard spreading (WH-S): a truncated $J\times K$ Walsh-Hadamard (WH) matrix;

(iii) Pseudonoise spreading (PN-S): a $J\times K$ matrix $\mathbf{\Theta}_\mu$ with $\pm 1, \pm j$ PN entries.

Blind or pilot-based channel estimation is needed for determining the multichannel equalizer $\mathbf{\Gamma}_\mu$. If CSI is available at the receiver, estimated symbols $\hat{\mathbf{s}}_\mu(i)$ are obtained at the output of $\mathbf{\Gamma}_\mu$ as

$$\hat{\mathbf{s}}_\mu(i) = \mathbf{\Gamma}_\mu \mathbf{y}_\mu(i). \tag{14}$$

Possible choices include the matched-filter (MF) receiver $\mathbf{\Gamma}_\mu = (\mathbf{D}_\mu(H_\mu)\mathbf{\Theta}_\mu)^{\mathcal{H}}$; the minimum mean-square error (MMSE) receiver

$$\mathbf{\Gamma}_\mu = \mathbf{\Theta}_\mu^{\mathcal{H}} \mathbf{D}_\mu^{\mathcal{H}}(H_\mu) \left(\mathbf{R}_{\eta_\mu} + \mathbf{D}_\mu(H_\mu)\mathbf{\Theta}_\mu\mathbf{\Theta}_\mu^{\mathcal{H}}\mathbf{D}_\mu^{\mathcal{H}}(H_\mu)\right)^{-1}, \tag{15}$$

where $\mathbf{R}_{\eta_\mu} := \mathrm{E}\{\boldsymbol{\eta}_\mu(i)\boldsymbol{\eta}_\mu^{\mathcal{H}}(i)\}$; and the ZF-receiver $\mathbf{\Gamma}_\mu = (\mathbf{D}_\mu(H_\mu)\mathbf{\Theta}_\mu)^\dagger$, which will guarantee ISI-free detection.

For Va-S, a blind channel estimation method was developed in [12]. In the sequel, we will establish identifiability conditions and derive a more general blind channel estimation algorithm allowing also Va-S, WH-S, or PN-S code matrices $\mathbf{\Theta}_\mu$.

5. BLIND CHANNEL ESTIMATION

We will suppose here that instead of (d1), we design $\mathbf{\Theta}_\mu$ such that

(d1′) *$J \geq K + L$ and any K rows of $\mathbf{\Theta}_\mu$ span the $\mathbb{C}^K$ row vector space.*

Note that when $J = J_{\min} = K + L$, (d1′) is equivalent to (d1). To estimate $\{h_\mu(l)\}_{l=0}^L$ under (d1′) in the noiseless case, the receiver corresponding to user μ collects N blocks of $\mathbf{y}_\mu(i)$ in a $J \times N$ matrix $\mathbf{Y}_\mu := [\mathbf{y}_\mu(0)\ \mathbf{y}_\mu(1)\ \cdots\ \mathbf{y}_\mu(N-1)]$ and forms $\mathbf{Y}_\mu\mathbf{Y}_\mu^{\mathcal{H}} = \mathbf{D}_\mu(H_\mu)\mathbf{\Theta}_\mu\mathbf{S}_\mu\mathbf{S}_\mu^{\mathcal{H}}\mathbf{\Theta}_\mu^{\mathcal{H}}\mathbf{D}_\mu^{\mathcal{H}}(H_\mu)$, where $\mathbf{S}_\mu := [\mathbf{s}_\mu(0)\ \mathbf{s}_\mu(1)\ \cdots\ \mathbf{s}_\mu(N-1)]_{K\times N}$. Receiver μ also chooses

(d2) *N large enough so that $\mathbf{S}_\mu\mathbf{S}_\mu^{\mathcal{H}}$ is of full rank K.*

Under (d1′) and (d2), we have rank $(\mathbf{Y}_\mu\mathbf{Y}_\mu^{\mathcal{H}}) = K$ and range space $\mathcal{R}(\mathbf{Y}_\mu\mathbf{Y}_\mu^{\mathcal{H}}) = \mathcal{R}(\mathbf{D}_\mu(H_\mu)\mathbf{\Theta}_\mu)$. Thus, the nullity of $\mathbf{Y}_\mu\mathbf{Y}_\mu^{\mathcal{H}}$ is $\nu(\mathbf{Y}_\mu\mathbf{Y}_\mu^{\mathcal{H}}) = J - K$. Further, the eigendecomposition

$$\mathbf{Y}_\mu\mathbf{Y}_\mu^{\mathcal{H}} = [\mathbf{U}, \tilde{\mathbf{U}}] \begin{bmatrix} \mathbf{\Sigma}_{K\times K} & \mathbf{0}_{K\times(J-K)} \\ \mathbf{0}_{(J-K)\times K} & \mathbf{0}_{(J-K)\times(J-K)} \end{bmatrix} \begin{bmatrix} \mathbf{U}^{\mathcal{H}} \\ \tilde{\mathbf{U}}^{\mathcal{H}} \end{bmatrix} \tag{16}$$

yields the $J \times (J - K)$ matrix $\tilde{\mathbf{U}}$ whose columns span the null space $\mathcal{N}(\mathbf{Y}_\mu\mathbf{Y}_\mu^{\mathcal{H}})$. Because the latter is orthogonal to $\mathcal{R}(\mathbf{Y}_\mu\mathbf{Y}_\mu^{\mathcal{H}}) = \mathcal{R}(\mathbf{D}_\mu(H_\mu)\mathbf{\Theta}_\mu)$, it follows that $\tilde{\boldsymbol{u}}_l^{\mathcal{H}}\mathbf{D}_\mu(H_\mu)\mathbf{\Theta}_\mu = \mathbf{0}_{1\times K}^T$, $l \in [1, J-K]$, where $\tilde{\boldsymbol{u}}_l$ denotes the lth column of $\tilde{\mathbf{U}}$. With $\mathbf{D}(\tilde{u}_l)$ denoting the diagonal matrix $\mathbf{D}(\tilde{u}_l) := \mathrm{diag}[\tilde{\boldsymbol{u}}_l^{\mathcal{H}}]$ and $\mathbf{d}(H_\mu) := [H_\mu(\rho^\mu)\ H_\mu(\rho^{\mu+M})\ \cdots\ H_\mu(\rho^{\mu+(J-1)M})]^T$, we can write $\tilde{\boldsymbol{u}}_l^{\mathcal{H}}\mathbf{D}_\mu(H_\mu) = \mathbf{d}^T(H_\mu)\mathbf{D}(\tilde{u}_l)$. It can be easily verified that with $\mathbf{h}_\mu := [h_\mu(0)\ h_\mu(1)\ \cdots\ h_\mu(L)]^T$ and with $\mathbf{V}_\mu$ being an $(L+1)\times J$ matrix whose $(l+1, j+1)$th entry is $\rho^{-l(\mu+jM)}$, one can write $\mathbf{d}^T(H_\mu) = \mathbf{h}_\mu^T\mathbf{V}_\mu$. This yields

$$\mathbf{h}_\mu^T\mathbf{V}_\mu \left[\mathbf{D}(\tilde{u}_0)\mathbf{\Theta}_\mu, \ldots, \mathbf{D}(\tilde{u}_{J-K})\mathbf{\Theta}_\mu\right] = \mathbf{0}_{1\times K(J-K)}^T, \tag{17}$$

from which one can solve for $\mathbf{h}_\mu$. The uniqueness (within a scale) in solving for $\mathbf{h}_\mu$ is established in Appendix B. If the noise $\boldsymbol{\eta}_\mu$ is colored and its covariance matrix is available, we can prewhiten $\mathbf{Y}_\mu$ before singular value decomposition (SVD), and a similar blind channel estimation algorithm can be devised. We summarize the symbol recovery conditions and the blind channel estimation result in the following.

Theorem 1. (i) *Design a GMC-CDMA system according to (d1), and suppose that CSI is available at the receiver using pilots. User symbols $\mathbf{s}_\mu(i)$ can then be always recovered with linear processing as in* (14)*, regardless of the constellation and the underlying frequency-selective multipath channels up to order L.*

(ii) *A GMC-CDMA system designed according to (d1′) and (d2) guarantees blind identifiability (within a scale) of channels $h_\mu(l)$ with maximum order L. The channel estimate is found by solving* (17) *for the null eigenvector.*

Note that unlike [10], even blind channel-irrespective symbol recovery is assured by Theorem 1, without bandwidth-consuming channel coding/interleaving, even with linear receiver processing (as opposed to the exponentially complex maximum-likelihood sequence estimation used in [10]).

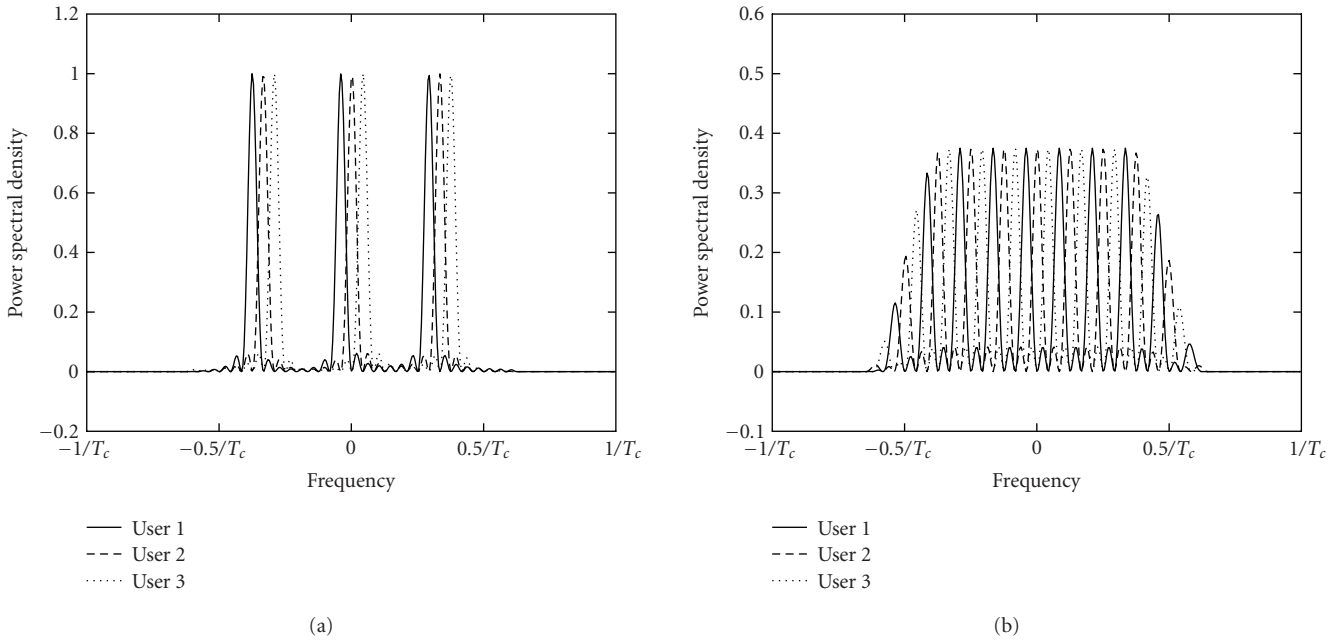

Figure 3: Power spectrum for $K = 2$, $L = 1$, and $\alpha = 0.3$: (a) $M = M_{\max} = 8$; (b) $M = 3$, $M_{\max} = 8$.

6. BANDWIDTH CONSIDERATIONS

In order to assess the spectrum characteristics of our system, we select a chip waveform $\psi(t)$ with root raised cosine spectrum $\Psi(f)$ and roll-off factor α. We suppose for simplicity that $s_{m,k}(i)$'s are uncorrelated for all $k \in [0, K-1]$ and for all $i \in \mathbb{Z}$. The power spectrum of the continuous-time transmitted GMC-CDMA signal $u_m(t)$ is

$$U_m(f) = \frac{|\Psi(f)|^2}{PT_c} \sum_{p=-P+1}^{P-1} \sum_{k=0}^{K-1} \sum_{i=0}^{P-1} c^*_{m,k}(i) c_{m,k}(p+i) e^{j2\pi f \cdot pT_c}. \tag{18}$$

In Figure 3a, we plot $U_m(f)$ for three users in a system with $M_{\max} = M = 8$, $K = 2$, $L = 1$, and $\alpha = 0.3$. The inner code $\mathbf{\Theta}_m$ is a $J \times K$ truncated WH-S matrix, while the outer-code matrix $\mathbf{F}_m$ is selected as in (9). The bandwidth B_{gmc} of GMC-CDMA is determined by the bandwidth of $\psi(t)$ which is approximately $1/T_c$, where $T_c = KT/P$. Therefore, the transmission bandwidth is $B_{\text{gmc}} = P/(KT)$ [Hz], and the normalized bandwidth efficiency (measured by the symbol rate to bandwidth ratio times the number of active users) is

$$\varepsilon = \frac{KM}{P} = \frac{KM}{M(K+L)+L}. \tag{19}$$

As mentioned in [12], GMC-CDMA is bandwidth efficient since in (19) $\varepsilon \to 1$ as we choose our block size $K \gg L$. Conventional multicarrier CDMA systems rely on channel coding and interleaving to combat errors due to MUI and ISI and overexpand bandwidth [10, 11], while our GMC-CDMA system relies on block spreading to deal with MUI and ISI. Of course, additional channel coding should be used on top of our block spreading to bring the error performance further down to the level prescribed by the intended application.

If the number of active users in the system decreases (say M goes from $M_{\max} = 8$ down to 3), we observe from Figure 3a that 5/8 of the total bandwidth is not utilized by the system. In this case only $1/M = 12.5\%$ of the total bandwidth available is assigned to each user. One way of taking advantage of the available bandwidth is to use a $J > J_{\min}$. By enlarging $\mathbf{\Theta}_m$ from $J_{\min} \times K$ to $J \times K$, we not only increase the number of transmit carriers ($J > J_{\min}$) per user (and thus increase the frequency diversity of our system), but also increase the amount of spreading for the K symbols in $\mathbf{s}_m(i)$ by using codes with spreading length J, both of which are beneficial to the system's performance. Supposing that we have the same total allocated bandwidth as in the full load scenario, we have $P/K = (M_{\max}J_{\min} + L)/K = (MJ + L)/K$. From the latter, we determine the number of subcarriers allocated to each of the active users as

$$J = \left\lfloor \frac{J_{\min}M_{\max}}{M} \right\rfloor. \tag{20}$$

The power spectral density for a GMC-CDMA system with $M_{\max} = 8$, $M = 3$, $K = 2$, $L = 1$, and $\alpha = 0.3$ is plotted in Figure 3b with the same parameters of Figure 3a, except that instead of $J_{\min} = K + L = 3$, we use $J = \lfloor J_{\min}M_{\max}/M \rfloor = 8$. We observe that the available bandwidth is now redistributed among the 3 active users. Unlike Figure 3a, we now assign $1/M = 33.3\%$ of the total bandwidth to each user.

In order to redistribute the available bandwidth to the active users, we allow the inner and outer precoders to change depending on the system load. Nevertheless, our transceivers

are designed to eliminate MUI and ISI deterministically and to guarantee symbol recovery for any number of users $M \in [1, M_{\max}]$. Given K, L, $M_{\max}$, and obtaining the number of active users M from the base station (BS), the mobiles can compute the number of subcarriers per user J from (20) and then use this value in (9) to obtain $\mathbf{F}_\mu$. The dimensionality of the inner precoding matrix $\mathbf{\Theta}_\mu$ is $J \times K$. If M changes, then J changes, and the mobiles have to adjust their inner spreading codes accordingly. Computation of $\mathbf{G}_\mu$ and $\mathbf{\Gamma}_\mu$ is performed at the BS which has knowledge of all system parameters.

7. SIMULATED PERFORMANCE

Theoretical bit error rate (BER) for GMC-CDMA with a ZF equalizer $\mathbf{\Gamma}_\mu = (\mathbf{D}_\mu(H_\mu)\mathbf{\Theta}_\mu)^\dagger$ was derived in [12] assuming perfect knowledge of the channel. Similar to [12], we choose for simplicity a binary phase-shift keying (BPSK) constellation to obtain in terms of the Q-function an average BER:

$$\bar{P}_e = \frac{1}{MK} \sum_{\mu=0}^{M-1} \sum_{k=0}^{K-1} Q\left(\sqrt{\frac{1}{\tilde{\mathbf{g}}_{\mu,k}^{\mathcal{H}} \tilde{\mathbf{g}}_{\mu,k} E_{\mu,k}}} \sqrt{\frac{2E_b}{N_0}} \right), \tag{21}$$

where $\tilde{\mathbf{g}}_{\mu,k}^{\mathcal{H}}$ is the kth row of matrix $\mathbf{\Gamma}_\mu \mathbf{G}_\mu$, $E_{\mu,k} := \sum_{i=0}^{P-1} |c_{\mu,k}(i)|^2$ is the energy of the μth user's kth code, and E_b/N_0 is the bit SNR.

For the GMC-CDMA system, we always choose the outer spreading matrix $\mathbf{F}_\mu$ as in (9). In the following test cases, we simulate uplink transmissions over frequency-selective channels. Each user experiences an FIR channel with $L+1$ taps selected to be independent and complex Gaussian distributed. We average the BER over 100 Monte Carlo channel realizations to avoid channel dependent performance.

Comparisons between different inner-spreadings $\mathbf{\Theta}_\mu$

In Figure 4, we plot (21) for GMC-CDMA using WH-S (i.e., WH inner-spreading $\mathbf{\Theta}_m = \mathbf{\Theta}$ for all $m \in [0, M-1]$), PN-S, and Va-S under different load conditions. The GMC-CDMA system is designed for $M_{\max} = 16$ users with symbols drawn from a BPSK constellation, each one experiencing a channel of order $L = 3$ assumed to be known at the receiver. The length of the $\mathbf{s}_\mu(i)$ blocks is $K = 8$. We decrease the number of active users from $M_{\max} = 16$ down to $M = 2$ and each time we select $J = \lfloor J_{\min} M_{\max}/M \rfloor$ (see Section 6) to incorporate the available bandwidth. When $M \in \{12, 14, 16\}$, we replace the WH-S matrix $\mathbf{\Theta}_\mu$ with a PN-S in order to satisfy condition (d1). If Va-S is used, we observe from Figure 4 that under different load conditions there is no difference in performance. It turns out that with matrix $\mathbf{\Theta}_\mu$ selected to be Va-S, we can write $\mathbf{C}_\mu = J\mathbf{f}_M^*(e^{j2\pi\mu/M}) \otimes [\mathbf{I}_K, \mathbf{0}_{K\times(J-K)}]^T$. When the number of active users M decreases, J increases, but this will only increase the number of all-zero rows of matrix $\mathbf{C}_\mu$, which explains why performance of the GMC-CDMA system will not improve in reduced load if a Va-S is used. This suggests that when load decreases in a GMC-CDMA system with Va-S, instead of redistributing the available bandwidth among active users following the procedure of Section 6, one can afford to use channel coding in order to improve error performance. Analysis of GMC-CDMA with channel coding is beyond the scope of this paper (see [22] for preliminary simulations and [13] for related studies in the single-user case[1]). Unlike Va-S, for WH-S and PN-S, the all-zero rows of matrix $\mathbf{C}_\mu$ do not increase with J and therefore frequency diversity increases with J. It is clear from Figure 4 that under 65% load the GMC-CDMA system with WH-S outperforms GMC-CDMA with Va-S.

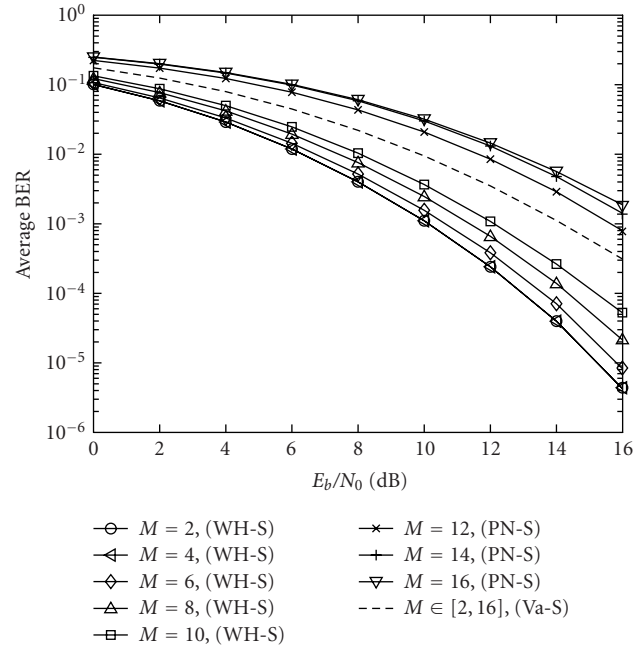

FIGURE 4: GMC-CDMA with Va-S, WH-S, and PN-S and different number of active users: theoretical performance with ZF receiver; $M_{\max} = 16$, $K = 8$, $L = 3$.

Comparisons with MC-CDMA, MC-DS-CDMA, MT- CDMA, and DS-CDMA

Here we compare GMC-CDMA with the single and multicarrier CDMA systems unified in Section 3. In Figure 5, the theoretical performance of GMC-CDMA with WH-S and $M_{\max} = 16$, $K = 8$, $L = 3$ is compared with an equivalent MC-CDMA system (see Section 3.1) using WH codes and OFDM transceivers with CP. The two systems have the same bandwidth; hence the MC-CDMA's WH code length is $J = \lfloor (J_{\min} M_{\max} + L)/K \rfloor - L = 19$. Both systems rely on a ZF-receiver that assumes perfect CSI. For a reduced load scenario, GMC-CDMA with a WH precoder has a lower BER than MC-CDMA. If WH-S is replaced by the OFDM-like Va-S when the system load increases over 65%, GMC-CDMA has better performance than MC-CDMA regardless of the number of active users. However, in light load MUI is less

[1] As GMC-CDMA eliminates MUI by design, the gap between uncoded and coded operation in the multiuser case is predicted accurately by the single-user comparisons in [13].

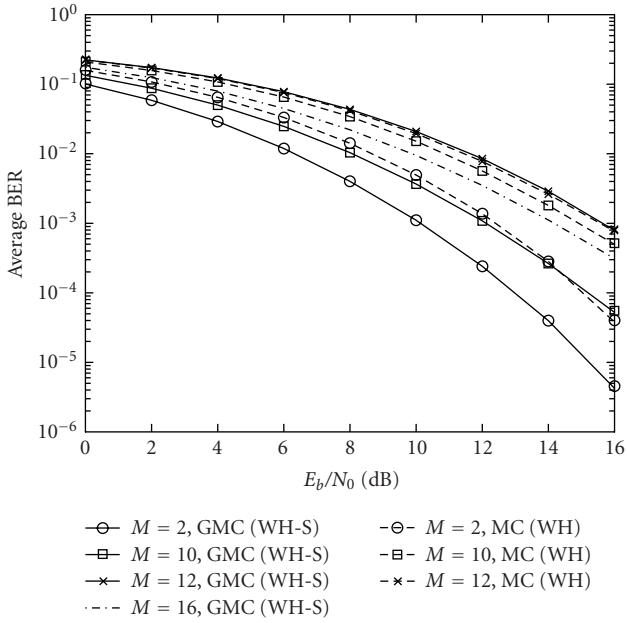

FIGURE 5: GMC-CDMA ($K = 8$) with WH-S and Va-S versus MC-CDMA with WH codes of length $J = 19$: theoretical performance with ZF receiver; $M_{\max} = 16$, $L = 3$.

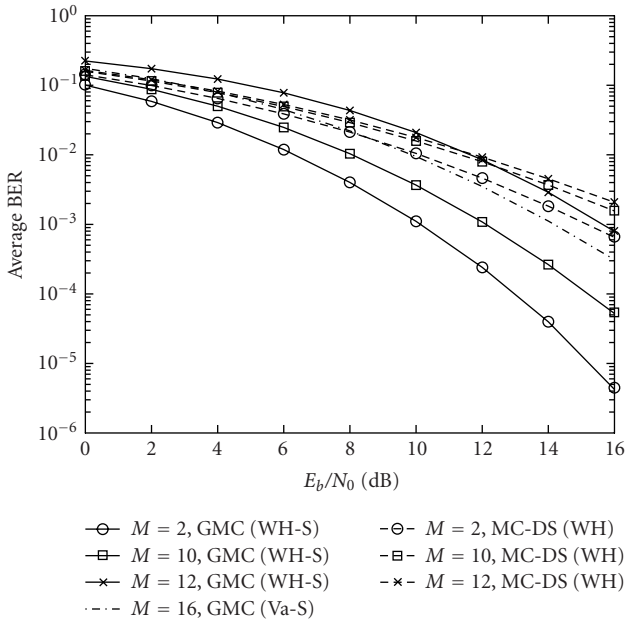

FIGURE 6: GMC-CDMA versus MC-DS-CDMA with $P = 179$, $\alpha = 0.2144$, $Q = 18$, and $\alpha_{\text{ds}} = 0.2$: theoretical performance with ZF receiver; $M_{\max} = 16$, $K = 8$, $L = 3$.

severe and MC-CDMA with WH codes is able to better combat channel fading, than a GMC-CDMA system with Va-S.

The average BER for MC-DS-CDMA with $f_k = k/T_{\text{ds}}$ and GMC-CDMA with WH-S, both using the same parameters as before and ZF-receivers, are compared in Figure 6. Block length $P = 179$ was used for both MC-DS-CDMA and GMC-CDMA in order for both systems to have the same transmission bandwidth. A WH spreading sequence of length $Q = 18$ is D/A converted and then pulse shaped with a raised cosine filter with roll-off factor $\alpha_{\text{ds}} = 0.2$ and spectral support $B_{\text{ds}} = (1 + \alpha_{\text{ds}})/T_{\text{ds}}$ to obtain $\theta_m(t)$. We select $\beta = 0.2127$ which leads to $P = (1 + \beta)Q(K + \alpha_{\text{ds}}) = 179$. The discrete-time spreading code $\boldsymbol{\theta}_m$ is obtained by sampling $\theta_m(t)$ every $T_c = T_{\text{ds}}/9.94$. We observe that in this case GMC-CDMA and also MC-CDMA outperform MC-DS-CDMA, regardless of the system load. Unlike MC-CDMA, where the information symbols ride on all subcarriers, in MC-DS-CDMA, different symbols are modulated on different subcarriers. Consequently, recovery of symbols modulated on subcarriers hit by channel nulls suffers more in MC-DS-CDMA.

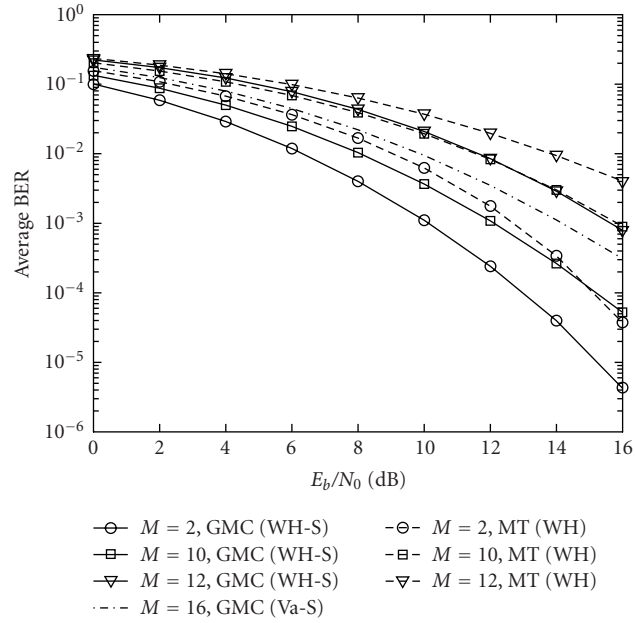

FIGURE 7: GMC-CDMA versus MT-CDMA with $P = 179$, $\alpha = 0.2127$, $Q = 117$, and $\alpha_{\text{ds}} = 0.2$: theoretical performance with ZF receiver; $M_{\max} = 16$, $K = 8$, $L = 3$.

Next, the same GMC-CDMA system is compared with MT-CDMA. The MT-CDMA system generates its spreading code $\boldsymbol{\theta}_m$ similar to MC-DS-CDMA. If we select $Q = 117$ and $\alpha_{\text{ds}} = 0.2$, then $P = (1 + \beta)((1 + \alpha_{\text{ds}})Q + K - 1) = 179$ implies $\beta = 0.2144$. The sampling period is now $T_c = T_{\text{ds}}/1.53$. The results plotted in Figure 7 show that GMC-CDMA outperforms MT-CDMA. We also observe that MT-CDMA performs similar to MC-CDMA in light load, but has a higher BER when $M = 12$ users are active out of $M_{\max} = 16$.

We also compare GMC-CDMA with $K = 8$, $L = 3$, $M_{\max} = 16$, and $M = 11$ against DS-CDMA with spreading $P = 19$ (chosen to ensure that the two systems occupy the same bandwidth). Both systems use WH codes. Figure 8 shows that GMC-CDMA outperforms DS-CDMA when MF or MMSE receivers are used. For the MMSE receiver, GMC-CDMA is an order of magnitude better than DS-CDMA in BER performance at $E_b/N_0 = 16$ dB.

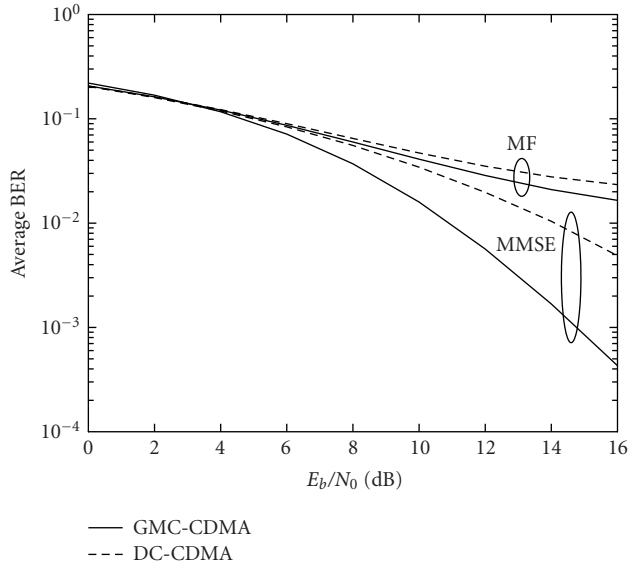

Figure 8: GMC-CDMA with $K = 8$ versus DS-CDMA with $P = 19$: simulations for MF and MMSE receivers; $M_{\max} = 16$, $M = 11$, $L = 3$.

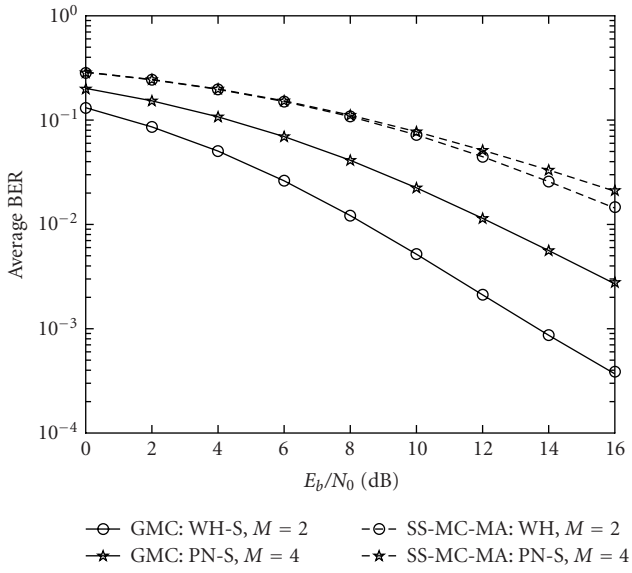

Figure 9: Theoretical performance for GMC-CDMA and SS-MC-MA; $M_{\max} = 4$, $K = 15$, $L = 2$.

Importance of checking condition (d1)

To stress out the importance of checking condition (d1), we compare in Figure 9 the performance of GMC-CDMA with $K = 15$ designed for $M_{\max} = 4$ maximum users and $L = 2$ with performance of an equivalent uncoded spread-spectrum multicarrier multiple-access (SS-MC-MA) system proposed in [10] with $M = 2$ and $M = 3$. The parameters of SS-MC-MA are selected such that it occupies the same transmission bandwidth as GMC-CDMA. Both systems use a ZF receiver. SS-MC-MA does not guarantee recovery of the transmit symbols (condition (d1) is not satisfied) and therefore performance suffers compared to GMC-CDMA.

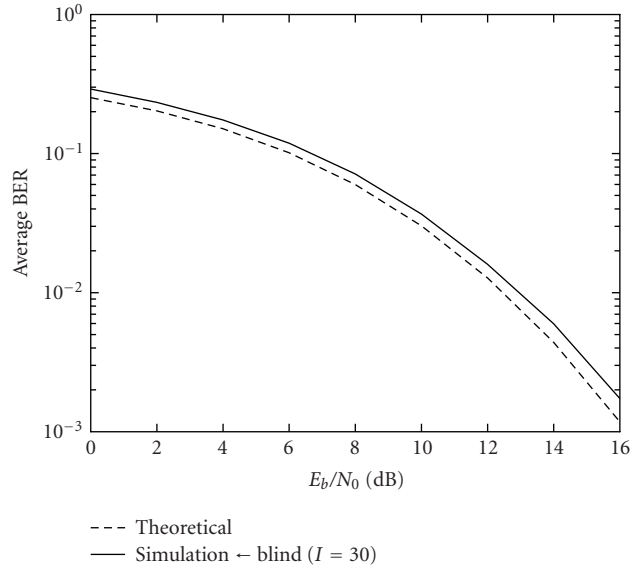

Figure 10: Blind GMC-CDMA with random codes and ZF receiver; $M = M_{\max} = 8$, $K = 8$, $L = 4$, $I = 30$.

Performance of the blind channel estimation algorithm

In the sequel, performance of the GMC-CDMA blind channel estimation algorithm is assessed by simulating a system that uses an inner-code matrix $\mathbf{\Theta}_m$ with equiprobable ± 1, $\pm 1j$ entries, designed with $K = 8$ and $L = 4$ for $M_{\max} = M = 8$ users. For blind channel estimation, we processed $I = 30$ size $P = 100$. The average BER is plotted in Figure 10 along with the theoretical BER curve obtained from (21). We infer from Figure 10 that GMC-CDMA is able to identify and estimate the channel reliably even at low SNR.

In the end, we want to point out that the inner- and outer-code changing operations at the mobile transmitters can be controlled by the BS, which has knowledge of the system load. If the outer precoder of the mobile users $\mathbf{F}_\mu$ is formed by equispaced exponentials as in (9), and if the BS assigns to each of the active users a different tag number μ between 1 and M, then it is enough for the BS to inform each of the mobile users of their tag μ and of the total number of active users M in the system for the mobile transmitters to be able to compute $\mathbf{F}_\mu$ and $\mathbf{\Theta}_\mu$. The assigned tag μ differentiates the mobiles and allows each of them to choose J different subcarriers out of the total MJ equispaced subcarriers, and consequently use (9) to compute $\mathbf{F}_\mu$. So, the BS has to send only two numbers (M and μ) to the mobiles when M changes. This is a small price to pay considering that one would gain, for the example presented in Figure 4, between 0 dB and 4 dB at BER$= 10^{-3}$ as M goes from $M_{\max} = 16$ to 2. It is not necessary to devise a new data link layer protocol as one can use the existing demand-assignment medium access control protocol of [23] to allow the base station to inform

the mobile users of their code assignment every time a user enters or exits the system. Changes in the load are treated like a modification of bandwidth requests from the mobile users.

8. CONCLUDING REMARKS

In this paper, we developed a GMC-CDMA system for wireless MUI/ISI resilient transmissions over frequency-selective channels. We showed that GMC-CDMA encompasses single-carrier DS-CDMA and several multicarrier CDMA systems, which allow us to implement the various options digitally as special cases. We also highlighted the symbol recovery problems in the uplink that are common to the existing multiple-access schemes. GMC-CDMA offers guarantees on symbol recovery with low-complexity linear receivers while keeping high bandwidth efficiency in both full load and underloaded settings. We also developed a novel blind channel estimation algorithm for general spreading codes. Simulations revealed the unifying framework, the generality, and the promising performance of GMC-CDMA relative to existing alternatives.

This paper focused on physical layer issues of GMC-CDMA under variable number of single-rate active users. For a GMC-CDMA system with *multirate* capabilities, the interested reader is referred to [19]. Error performance of GMC-CDMA with linear and ZF decision-feedback receivers has been analyzed in [22]. Also in [23], an integrated multirate GMC-CDMA system is designed to account for the data link, medium access control and physical layer issues. Multiple access design issues for doubly selective channels have been dealt with in [24, 25], and a group-orthogonal multicarrier CDMA scheme is proposed in [26]. Future research directions include further comparisons along the lines of [23] and suppression of narrowband and cochannel interference.

APPENDICES

A. PROOF OF $\mathbf{G}_{\text{tz}}^{(1)}\mathbf{H}_m\mathbf{F}_{\text{tz}} = \mathbf{D}_m(H)$

From the definition of $\mathbf{F}_{\text{tz}}$ and $\mathbf{G}_{\text{tz}}^{(1)}$, we can write $\mathbf{F}_{\text{tz}} = \mathbf{I}_2\mathbf{F}_J := [\mathbf{I}_J, \mathbf{0}_{J\times L}]\mathbf{F}_J$ and

$$\mathbf{G}_{\text{tz}}^{(1)} = \mathbf{F}_J^{\mathcal{H}}\mathbf{I}_1 := \mathbf{F}_J^{\mathcal{H}}\begin{bmatrix}\mathbf{I}_J & \vdots & \mathbf{I}_L \\ & \vdots & \mathbf{0}_{(J-L)\times L}\end{bmatrix}. \tag{A.1}$$

Thus, we have $\mathbf{G}_{\text{tz}}^{(1)}\mathbf{H}_m\mathbf{F}_{\text{tz}} = \mathbf{F}_J^{\mathcal{H}}\mathbf{I}_1\mathbf{H}_m\mathbf{I}_2\mathbf{F}_J$. Substituting $\mathbf{I}_1$'s and $\mathbf{I}_2$'s definitions into $\mathbf{I}_1\mathbf{H}_m\mathbf{I}_2 := \overset{\circ}{\mathbf{H}}_m$, we can verify that $\overset{\circ}{\mathbf{H}}_m$ is a $J \times J$ circulant matrix with (k,l)th entry $h_m((k-l) \bmod J)$. It is shown in [27, page 202] that by multiplying a $J\times J$ circulant matrix with $\mathbf{F}_J^{\mathcal{H}}$ from the left and with $\mathbf{F}_J$ from the right, the diagonal matrix $\mathbf{D}_m(H)$ is obtained with its diagonal entries corresponding to the FFT of the first column of $\overset{\circ}{\mathbf{H}}_m$. This concludes our proof.

B. PROOF OF THE UNIQUENESS OF $\mathbf{h}_\mu$ IN (17)

To prove the uniqueness (up to a complex constant) of $\mathbf{h}_\mu$ in (17), we only need to show that if two channels $\mathbf{h}_m$ and $\mathbf{h}_\mu$ result in the same signal subspace, that is,

$$\mathbf{D}_m(H_m)\mathbf{\Theta}_\mu = \mathbf{D}_\mu(H_\mu)\mathbf{\Theta}_\mu\mathbf{A}, \tag{B.1}$$

where $\mathbf{A}$ is a full rank $K\times K$ matrix, then $\mathbf{D}_m(H_m) = \lambda\mathbf{D}_\mu(H_\mu)$ and $\mathbf{A} = \lambda\mathbf{I}_K$, where λ is a constant. We will only prove this for the case $J = K+L$. When $J > K+L$, one can simply select any $K+L$ rows of $\mathbf{D}_m(H_m)\mathbf{\Theta}_\mu$ and $\mathbf{D}_\mu(H_\mu)\mathbf{\Theta}_\mu$ and apply the proof for the $J = K+L$ case.

First, we can see from (B.1) that if $\mathbf{D}_\mu(H_\mu)$ has a zero (j,j)th entry, the (j,j)th entry of $\mathbf{D}_m(H_m)$ must also be zero. If $\mathbf{D}_\mu(H_\mu)$ has L zero entries, then $\mathbf{D}_m(H_m)$ will also have L entries at the same locations. This means that $\{H_m(\rho^n)\}$ and $\{H_\mu(\rho^n)\}$ will have the same L roots. In this case, we must have $\mathbf{h}_\mu = \alpha\mathbf{h}_m$.

If $\mathbf{D}_\mu(H_\mu)$ has less than L zero entries, without loss of generality, we can assume the first $K+1$ entries of $\mathbf{D}_\mu(H_\mu)$ (and hence of $\mathbf{D}_m(H_m)$) are nonzero. Let $\boldsymbol{\theta}_{\mu,j}^T$ denote the jth row of $\mathbf{\Theta}_\mu$. Defining $\lambda_j := H_m(\rho^{m+(j-1)M})/H_\mu(\rho^{\mu+(j-1)M})$, one can write (B.1) as

$$\lambda_j\boldsymbol{\theta}_{\mu,j}^T = \boldsymbol{\theta}_{\mu,j}^T\mathbf{A}, \quad j = 1,\ldots,K+1, \tag{B.2}$$

which means that for $1 \le j \le K+1$, $\boldsymbol{\theta}_{\mu,j}$ is an eigenvector of $\mathbf{A}^T$ and λ_j is the corresponding eigenvalue. To prove that $\mathbf{A} = \lambda\mathbf{I}_K$ for some λ, we need to show that $\mathbf{A}$ (and hence $\mathbf{A}^T$) has identical eigenvalues. We prove this by contradiction. Suppose $\mathbf{A}^T$ has two or more different eigenvalues. Then we can always divide its eigenvalues $\{\lambda_j\}_{j=1}^{K+1}$ into two nonoverlapping groups such that there is no common eigenvalue between the two groups. Neither of the two groups will have more than K eigenvalues. By the assumption that any K rows of $\mathbf{\Theta}_\mu$ are linear independent (c.f. (d2')), the eigenvectors corresponding to the first (or the second) group must be independent of each other. But eigenvectors corresponding to different eigenvalues should be linearly independent. Therefore, the eigenvectors corresponding to the first group should be linearly independent of the eigenvectors corresponding to the second group. This way, we have found a total of $K+1$ linearly independent eigenvectors $\{\boldsymbol{\theta}_{\mu,j}\}_{j=1}^{K+1}$ of a $K\times K$ matrix $\mathbf{A}^T$, which is impossible.

Therefore, all the eigenvalues $\{\lambda_j\}_{j=1}^{K+1}$ should be the same, which means that $\mathbf{A} = \lambda\mathbf{I}_K$ for some constant λ. It follows that $\mathbf{D}_m(H_m) = \lambda\mathbf{D}_\mu(H_\mu)$ and $\mathbf{h}_m = \lambda\mathbf{h}_\mu$.

ACKNOWLEDGMENTS

This work was supported by the NSF Wireless Initiative Grant no. 99-79443. The original version was submitted to the EURASIP Journal on Applied Signal Processing, January 28, 2004. Part of this paper was presented at the Second MultiCarrier Spread-Spectrum Workshop (MCSS '99) and at the International Conference on Acoustics, Speech, and Signal Processing (ICASSP '00).

REFERENCES

[1] R. Van Nee and R. Prasad, *OFDM for Wireless Multimedia Communications*, Artech House Publishers, London, UK, 2000.

[2] L. J. Cimini, "Analysis and simulation of a digital mobile channel using orthogonal frequency division multiplexing," *IEEE Trans. Commun.*, vol. 33, no. 7, pp. 665–675, 1985.

[3] V. M. DaSilva and E. S. Sousa, "Multicarrier orthogonal CDMA signals for quasi-synchronous communication systems," *IEEE J. Select. Areas Commun.*, vol. 12, no. 5, pp. 842–852, 1994.

[4] K. Fazel, "Performance of CDMA/OFDM for mobile communication system," in *Proc. 2nd IEEE International Conference on Universal Personal Communications (ICUPC '93)*, vol. 2, pp. 975–979, Ottawa, Ontario, Canada, October 1993.

[5] S. Hara and R. Prasad, "Overview of multicarrier CDMA," *IEEE Commun. Mag.*, vol. 35, no. 12, pp. 126–133, 1997.

[6] S. Kondo and L. B. Milstein, "Performance of multicarrier DS CDMA systems," *IEEE Trans. Commun.*, vol. 44, no. 2, pp. 238–246, 1996.

[7] L. Vandendorpe, "Multitone spread spectrum multiple access communications system in a multipath Rician fading channel," *IEEE Trans. Veh. Technol.*, vol. 44, no. 2, pp. 327–337, 1995.

[8] N. Yee, J.-P. Linnartz, and G. Fettweis, "Multicarrier CDMA in indoor wireless radio networks," in *Proc. 4th IEEE International Symposium on Personal, Indoor and Mobile Radio Communications (PIMRC '93)*, pp. 109–113, Yokohama, Japan, September 1993.

[9] Q. Chen, E. S. Sousa, and S. Pasupathy, "Performance of a coded multi-carrier DS-CDMA system in multipath fading channels," *Wireless Personal Communications Journal*, vol. 2, no. 1-2, pp. 167–183, 1995.

[10] S. Kaiser and K. Fazel, "A spread spectrum multi-carrier multiple access system for mobile communications," in *Proc. 1st International Workshop on Multi-Carrier Spread-Spectrum (MC-SS '97)*, pp. 49–56, Oberpfaffenhofen, Germany, April 1997.

[11] D. Rowitch and L. Milstein, "Convolutionally coded multicarrier DS-CDMA systems in a multipath fading channel-I. Performance analysis," *IEEE Trans. Commun.*, vol. 47, no. 10, pp. 1570–1582, 1999.

[12] G. B. Giannakis, Z. Wang, A. Scaglione, and S. Barbarossa, "AMOUR-generalized multicarrier transceivers for blind CDMA regardless of multipath," *IEEE Trans. Commun.*, vol. 48, no. 12, pp. 2064–2076, 2000.

[13] Z. Wang and G. B. Giannakis, "Complex-field coding for OFDM over fading wireless channels," *IEEE Trans. Inform. Theory*, vol. 49, no. 3, pp. 707–720, 2003.

[14] A. Scaglione, G. B. Giannakis, and S. Barbarossa, "Redundant filterbank precoders and equalizers-part II: blind channel estimation, synchronization, and direct equalization," *IEEE Trans. Signal Processing*, vol. 47, no. 7, pp. 2007–2022, 1999.

[15] S. Verdú, "Wireless bandwidth in the making," *IEEE Commun. Mag.*, vol. 38, no. 7, pp. 53–58, 2000.

[16] Z. Wang and G. B. Giannakis, "Block spreading for multipathresilient generalized multi-carrier CDMA," in *Signal Processing Advances in Wireless and Mobile Communications*, G. B. Giannakis, Y. Hua, P. Stoica, and L. Tong, Eds., vol. 2, chapter 9, Prentice-Hall, Englewood Cliffs, NJ, USA, 2000.

[17] Z. Wang and G. B. Giannakis, "Wireless multicarrier communications: where Fourier meets Shannon," *IEEE Signal Processing Mag.*, vol. 17, no. 3, pp. 29–48, 2000.

[18] K. Fazel and L. Papke, "On the performance of convolutionally-coded CDMA/OFDM for mobile communication system," in *Proc. 4th IEEE International Symposium on Personal, Indoor and Mobile Radio Communications (PIMRC '93)*, pp. 468–472, Yokohama, Japan, September 1993.

[19] Z. Wang and G. B. Giannakis, "Block precoding for MUI/ISI-resilient generalized multicarrier CDMA with multirate capabilities," *IEEE Trans. Commun.*, vol. 49, no. 11, pp. 2016–2027, 2001.

[20] A. Scaglione, G. B. Giannakis, and S. Barbarossa, "Lagrange/Vandermonde MUI eliminating user codes for quasi-synchronous CDMA in unknown multipath," *IEEE Trans. Signal Processing*, vol. 48, no. 7, pp. 2057–2073, 2000.

[21] S. Ohno, P. A. Anghel, G. B. Giannakis, and Z.-Q. Luo, "Multicarrier multiple access is sum-rate optimal for block transmissions over circulant ISI channels," in *Proc. IEEE Conference on Communications (ICC '02)*, pp. 1656–1660, New York, NY, USA, April–May 2002.

[22] G. B. Giannakis, A. Stamoulis, Z. Wang, and P. A. Anghel, "Load-adaptive MUI/ISI-resilient generalized multi-carrier CDMA with linear and DF receivers," *European Trans. Telecommunications*, vol. 11, no. 6, pp. 527–537, 2000.

[23] A. Stamoulis and G. B. Giannakis, "Packet fair queueing scheduling based on multirate multipath-transparent CDMA for wireless networks," in *Proc. 19th Annual Joint Conference of the IEEE Computer and Communications Societies (INFOCOM '00)*, vol. 3, pp. 1067–1076, Tel Aviv, Israel, March 2000.

[24] G. Leus, S. Zhou, and G. B. Giannakis, "Orthogonal multiple access over time- and frequency-selective channels," *IEEE Trans. Inform. Theory*, vol. 49, no. 8, pp. 1942–1950, 2003.

[25] X. Ma and G. B. Giannakis, "Maximum-diversity transmissions over doubly selective wireless channels," *IEEE Trans. Inform. Theory*, vol. 49, no. 7, pp. 1832–1840, 2003.

[26] X. Cai, S. Zhou, and G. B. Giannakis, "Group-orthogonal multicarrier CDMA," *IEEE Trans. Commun.*, vol. 52, no. 1, pp. 90–99, 2004.

[27] G. H. Golub and C. F. Van Loan, *Matrix Computations*, Johns Hopkins University Press, Baltimore, Md, USA, 3rd edition, 1996.

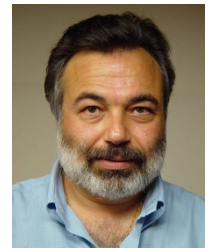

Georgios B. Giannakis received his B.S. in electrical engineering in 1981 from the National Technical University of Athens, Greece, and his M.S. and Ph.D. degrees in electrical engineering in 1983 and 1986 from the University of Southern California. Since 1999, he has been a Professor in the Department of Electrical and Computer Engineering, the University of Minnesota, where he now holds an Endowed ADC Chair in wireless telecommunications. His general interests span the areas of communications and signal processing, estimation and detection theory—subjects on which he has published more than 200 journal papers, 350 conference papers, and two edited books. Current research focuses on complex-field and space-time coding, multicarrier, ultra-wideband wireless communication systems, cross-layer designs, and wireless sensor networks. He is the (co-) recipient of six best paper awards from the IEEE Signal Processing (SP) and Communications Societies (1992, 1998, 2000, 2001, 2003, 2004) and also received the SP Society's Technical Achievement Award in 2000. He is an IEEE Fellow since 1997, and has served the IEEE in various editorial and organizational posts.

Paul A. Anghel has received his B.S. degree in electrical engineering from the Polytechnic Institute of Bucharest in 1997 and his M.S. degree in electrical engineering from the University of Virginia in 2000. He is now a Ph.D. candidate in the Electrical and Computer Engineering Department, University of Minnesota. His interests lie in the area of multihop communication theory, data networks, and signal processing applications for wireless communication. Specific research interests include cooperative networks, space-time coding for distributed MIMO systems, information theoretic limits of multihop communication, and cross-layer design.

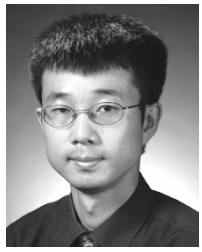

Zhengdao Wang was born in Dalian, China, in 1973. He received his B.S. degree in electrical engineering and information science from the University of Science and Technology of China (USTC), 1996, the M.S. degree in electrical and computer engineering from the University of Virginia, 1998, and the Ph.D. degree in electrical and computer engineering from the University of Minnesota, 2002. He is now in the Department of Electrical and Computer Engineering, the Iowa State University. His interests lie in the areas of signal processing, communications, and information theory.